DEUTSCHES ELEKTRONEN-SYNCHROTRON

DESY 94-041
March 1994

Some Aspects of Pion Physics in the Nambu- and Jona-Lasinio Model and Chiral Lagrangians

R. Tegen

Deutsches Elektronen-Synchrotron DESY, Hamburg

ISSN 0418-9833

NOTKESTRASSE 85 - 22603 HAMBURG

To be sure that your preprints are promptly included in the
HIGH ENERGY PHYSICS INDEX,
send them to (if possible by air mail):

DESY **Bibliothek** **Notkestraße 85** **22603 Hamburg** **Germany**	**DESY-IfH** **Bibliothek** **Platanenallee 6** **15738 Zeuthen** **Germany**

DESY 94-041
March 1994

ISSN 0418-9833

Some Aspects of Pion Physics in the Nambu–and Jona–Lasinio Model and Chiral Lagrangians

*Rudolph Tegen**

Deutsches Elektronen Synchrotron DESY

Notkestrasse 85, D–22603 Hamburg (Germany)

Abstract:

I discuss here to what extent the original two–flavour NJL model (which has a *minimal* number of adjustable parameters) reproduces pion observables. In particular, the sensitivity of the recently calculated electromagnetic mass shift to these NJL parameters is pointed out and a new way to fix them is suggested. A new set of $O(1/N_c)$ diagrams, which are the first meson loop corrections to the RPA, is presented and its effect on the pionic Goldstone mode, its electromagnetic form factor, weak decay constant, and on the constituent quark mass m is discussed. The relation of these NJL model results to some other chiral Lagrangians is pointed out, where ever possible. The here presented higher order diagrams indicate how one could systematically generate the next–order diagrams. It is, however, questionable whether the simplistic but mathematically manageable *contact* interaction of the NJL model should be maintained also in these higher order diagrams.

*Permanent address: Physics Department, Univ. Witwatersrand, P.O. Wits, Johannesburg 2050 (South Africa).

I. Introduction

The lightest hadron, the pseudoscalar pion $\pi^0(135)$, is almost 60 years after its invention by Yukawa in 1935 and 43 years after its experimental detection by Steinberger's group, still far from being completely understood. The reason is mainly that the theory of strong interactions, quantum chromodynmics (QCD), is quite difficult to quantify in the low–energy region. This is probably so *not* because of intrinsic *confinement* forces but rather because of the dynamical (or spontaneous) breaking of the underlying symmetry which gives rise to non–perturbative effects. At least one *non*–confining model exists which dynamically breaks the QCD gauge symmetries (i.e. changes its ground state) and satisfactorily describes the low–energy parameters of the pion. It is this link of the pion to the complexities of the interacting QCD ground state which makes the study of the humble pion even nowadays still rewarding. To illucidate the pion's role in the interacting vacuum's transition to a new phase (chirally symmetric phase with order parameter $< \bar{\psi}\,\psi >_0 = 0 \rightarrow$ chirally broken phase with $< \bar{\psi}\,\psi > \neq 0$) we recall the relevant processes in many–body physics. Consider the description of Ferromagnetism by the Ginzburg–Landau theory. For $T > T_c$ (Curie temperature) the ground state (g.s.) is rotationally invariant while for $T < T_c$ spontaneous magnetization sets in and breaks the rotational symmetry.

In condensed matter physics the BCS g.s. is a condensate of Cooper pairs (due to the spontaneous breaking of electromagnetic gauge symmetry which is triggered by the lattice phonon–mediated correlation between the opposite–spin electron pairs). In particle physics the QCD g.s. is a condensate of *scalar* quark–antiquark pairs (due to the dynamical breaking of chiral symmetry in the g.s. ; the rôle of the phonons is played here presumably by the gluons and *scalar* pairs are preferred because the vacuum is invariant under parity transformations). In dense nuclear matter a new g.s. could be formed under certain conditions (high temperature, large baryon number density and conservation of

certain flavour symmetry numbers like strangeness, as they might occur in neutron stars); this new g.s. would then be a condensate of *pseudoscalar* nucleon–hole intermediate states (again due to chiral symmetry breaking; now isovector pseudoscalar pionic modes are amplified in the nuclear medium and form a "pion condensate"). The importance of the dynamical breaking pattern of continuous gauge symmetries has recently been emphasized in connection with the "dynamical Higgs mechanism": the dynamical breaking of electroweak SU(2) ⊗ U(1) gauge symmetries can generate masses for the W and Z bosons without elementary Higgs scalars [1]. Dynamical symmetry breaking is an inherently non–perturbative effect and leads in certain models to the high collectivity of the pionic mode. As mentioned above the non–perturbative infrared domain is not straight–forwardly accessible to QCD proper. Numerical Monte Carlo simulations of the functional integral in a lattice regularized version of QCD have improved considerably in recent years [2,3]. Even meson and baryon form factors outside the immediate vicinity of $q^2 = 0$ have been reported with relatively small "error bars" [3]. Previous objections seem to have been overcome, that the pion can not be calculated in a completely realistic manner in which quarks of small but non–vanishing mass move in a large lattice volume with lattice spacings fine enough to guarantee asymptotic scaling. A common approximation that significantly reduces the numerical demands of the simulations is the "quenched approximation" which, however, might give results which are in conflict with the standard predictions of chiral perturbation theory. In particular, the chiral limit is problematic in all these simulations. In my view, the chiral limit is not only of academic interest but allows to simply relate certain observables via the powerful theorems of current algebra.

As an alternative, effective chiral theories such as NJL type models have been formulated in order to simulate in an approximate but explicit way QCD in the infrared domain. This domain is where pion physics is all–important. Here chiral symmetry and its breaking play a fundamental role in both low–energy strong and weak interactions, at both the hadron and quark levels. For a successful description of the

low–energy pion observables several conditions have to be met :

(i) the effective Lagrangian must have the same symmetries as QCD ($U_v(1)$ x $SU(2)_L$ x $SU(2)_R$ x $SU(N_c)_v$ x G where G stands for the discrete symmetries C,P,T);

(ii) the model must break chiral symmetry in the same way as does QCD, i.e. it must include genuine non–perturbative effects;

(iii) the model must be fully relativistic;

(iv) there must be no spurious center–of–mass motion of the composite particles (like the pion)

(v) the theory must be asymptotically free

Notably, conditions (i) – (iv) can be met without touching the confinement issue !

We discuss here mainly one model, the NJL model, which meets naturally all conditions (i) – (iv), and meets condition (v) after regularization (in a discontinuous way). Although there is a general analogy with the Cooper pairs of the BCS theory, there are also differences : if these NJL quark–antiquark pairs are embedded in an E– or B–field, the order parameter $m \sim < \bar{\psi}\,\psi >_0$ goes rapidly to zero if an *electric* field is applied (contrary to the behaviour exhibited by the Cooper pairs) but increases monotonically for magnetic field strength away from zero. As a result $m_\sigma(B)$ increases, $m_\sigma(E)$ decreases. The effect on m_π is much milder : $m_\pi(E)$ increases and converges towards $m_\sigma(E)$ while $m_\pi(B)$ increases only slightly. In the NJL model the cut–off Λ "enforces" asymptotic freedom; its ratio with the constituent quark mass m, (Λ/m), can, in principle, lie on two different branches: in the limit $(\Lambda/m) \to 0$ one recovers the non–linear sigma model (no σ–meson, no quarks) while the limit $(\Lambda/m) \to \infty$ gives $g_{\pi qq} \to 0$ and recovers the linear sigma model. If one fits (Λ/m) to f_π and Δm_π^2 one eliminates the high–mass branch of the original Fermi–Yang interpretation of the NJL model and finds (Λ/m) of order 4, more in line with the quark model interpretation of NJL. Therefore, the NJL model can only in an approximate sense be related to the sigma

model; this is also apparent from the absence of sea–gull diagrams in the gauged purely Fermionic NJL Lagrangian. Sea–gull and tadpole diagrams appear only upon "shrinking" of certain Fermion loop diagrams, hence they have a rich structure in the un–touched NJL model. In a symmetry preserving (Ward identities) way the sigma model is only concerned with the leading singularity of the NJL loop diagrams.

This article is organized as follows. In section II we present the two–flavour NJL model, its symmetries, dynamical breaking mechanism, and the dynamical generation of bound–state modes : $\vec{\pi}$, σ_o, η', $\vec{\sigma}_1$. Section III is devoted to the discussion of pion observables (f_π, constituent quark mass m, $< \bar{\psi}\ \psi >_o$, pion propagator for composite pions, $F_\pi(q^2)$, $\pi^o \to \gamma\gamma$ decay, α_π and β_π, $\Delta\, m_\pi{}^2$, $\rho_\pi(r)$, we ignore rare pion decays here) in leading and in sub–leading order in the number of colors, N_C; the chiral limit is particularly emphasized in part A in terms of several theorems, non–chiral corrections to $F_\pi(q^2)$ and $\Delta m_\pi{}^2$ are dealt with in part B where also some other pseudoscalar mass shifts are shown to be largely due to $\Delta m_\pi{}^2$ and to a SU(3) and SU(2) breaking parameter ratio. Section IV, finally, contains my conclusions.

II The two–flavour NJL model

The original two–flavour NJL Lagrangian [4].

$$\mathcal{L}_{NJL} = \bar{\psi}[i\partial^\mu\gamma_\mu - m_o]\psi + G[(\bar{\psi}\psi)^2 + (\bar{\psi}\, i\gamma_5\vec{\tau}\psi)^2] \qquad (2.1)$$

is (for $m_o \equiv 0$) invariant under $U_V(1) \otimes SU_L(2) \otimes SU_R(2) \otimes SU_V(N_C)$. The current quark mass matrix $m^o = \frac{1}{2}(m_u{}^o + m_d{}^o) + \frac{1}{2}\tau_3(m_u{}^o - m_d{}^o)$ breaks chiral symmetry explicitly. Here ψ is the quark field iso–dublett and colour–triplet and $\vec{\tau}$ are the isospin Pauli matrices. Note that here "colour" is not a *dynamical* degree of freedom (which is usually thought to be responsible for the confining forces of QCD) but rather a book–keeping device. Although the pion in this model will turn out to be the maximally bound (binding energy equals twice the constituent quark mass) Goldstone mode of

spontaneous chiral symmetry breaking, the constituents (quarks and antiquarks) are not confined "inside" the pion. The success of the NJL model for the low–energy properties of (in particular) the pion suggests that to a much lesser extent does the confinement issue determine low–energy parameters compared to the (apparently much more important) underlying symmetries of QCD, their spontaneous break–down, and the inclusion of non–perturbative effects.

The Lagrangian in eq (2.1) breaks $U_A(1)$ in the *maximal* fashion; to see this one can split $\mathcal{L}_{NJL}$ into the sum of the $U_L(2) \otimes U_R(2)$ symmetric term and the $U_A(1)$ breaking 't Hooft term (which here is a $2N_f = 4$ – Fermion interaction)

$$\mathcal{L}_{NJL} = \bar{\psi}(i\partial^\mu\gamma_\mu - m^o)\psi + \frac{G_1}{2}[(\bar{\psi}\psi)^2 + (\bar{\psi}\vec{\tau}\,\psi)^2 + + (\bar{\psi}\, i\psi_5\psi)^2 + (\bar{\psi}\, i\gamma_5\vec{\tau}\,\psi)^2] \qquad (2.2)$$

$$+ \frac{G_2}{2}[(\bar{\psi}\psi)^2 - (\bar{\psi}\vec{\tau}\,\psi)^2 - (\bar{\psi}\, i\gamma_5\psi)^2 + (\bar{\psi}\, i\gamma_5\vec{\tau}\psi)^2]$$

with equal coupling constants $G_1 = G_2$. The second term was derived by 't Hooft [5] directly from QCD and can be equivalently written in the familiar form:

$$\mathcal{L}_{'t\ Hooft} = G_2[\det\bar{\psi}(1+\gamma_5)\psi + \det\bar{\psi}(1-\gamma_5)\psi] \qquad (2.3)$$

More insight into the particle content of this theory is gained by rewriting (2.1) and (2.3) with

$$\sigma_o \equiv \bar{\psi}\psi,\ \vec{\sigma}_1 \equiv \bar{\psi}\vec{\tau}\,\psi,\ \eta' \equiv \bar{\psi}\, i\gamma_5\psi,\ \vec{\pi} \equiv \bar{\psi}\, i\gamma_5\vec{\tau}\,\psi \qquad (2.4)$$

$$\mathcal{L}_{NJL} = \bar{\psi}(i\partial^\mu\gamma_\mu - m_o)\psi + \frac{G_1}{2}[\sigma_o{}^2 + \vec{\pi}^2 + \eta'^2 + \vec{\sigma}_1{}^2]$$

$$+ \frac{G_1}{2}[\sigma_o{}^2 + \vec{\pi}^2 - \eta'^2 - \vec{\sigma}_1{}^2] \qquad (2.5)$$

The U_A (1) symmetry can be visualized for $N_f = 2$ as a rotation in an abstract "particle space" which naturally leaves the "length" of the particle vector $(\sigma_o, \vec{\pi}, \eta', \vec{\sigma}_1)$ invariant. Chiral symmetry is then a rotation in a particle subspace which leaves the length of the subvector $(\sigma_o, \vec{\pi})$ and $(\eta', \vec{\sigma}_1)$ invariant.

In the original publication [4] Nambu and Jona–Lasinio provided the leading (in the number of colours, N_c) non–perturbative approximation scheme that is consistent with the underlying chiral symmetry of their model. It is defined by two Schwinger–Dyson integral equations (Fig.1): (i) the one–body, or gap† equation with selfenergies (Fig. 1a,b) determined self–consistently, and (ii) the two–body, or Bethe–Salpeter bound state equation (Fig. 1c). This approximation is also known as "Hartree" (Fig. 1a), or "Hartree–Fock" (H–F) approximation (Fig. 1a+b) to the gap equation, and ladder or random phase approximation (RPA) for the two–body equation (Fig. 1c).

The RPA is known to preserve the symmetries of the underlying Lagrangian; there is, in particular, no center–of–mass problem with the bound–states of this approximation.

The position of the pole in the two–body propagator determines the mass of the bound state. This Lagrangian leads to a coupled set of gap equations

$$m_u = 4\,i\,N_c N_F G_1 \int^{\Lambda} \frac{d^4p}{(2\pi)^4} \frac{m_u}{p^2 - m_u^2} + 4\,i\,N_c N_F G_2 \int^{\Lambda} \frac{d^4p}{(2\pi)^4} \frac{m_d}{p^2 - m_d^2} \qquad (2.6)$$

†)This name originates from the formal similarity to the gap equation in the BCS theory of super–conductivity [6]. This analogy will be discussed further below.

$$m_d = 4i\,N_c N_F G_1 \int^{\Lambda} \frac{d^4p}{(2\pi)^4} \frac{m_d}{p^2 - m_d^2} + 4\,i\,N_c N_F G_2 \int^{\Lambda} \frac{d^4p}{(2\pi)^4} \frac{m_u}{p^2 - m_u^2}$$

in the chiral limit. These coupled equations have asymmetric solutions, but only in the $\Lambda \leq m$ region*). Hence they reduce to a single equal mass equation.

$$m = 4\,i\,N_c\,(G_1 + G_2) \int^{\Lambda} \frac{d^4p}{(2\pi)^4} \frac{m}{p^2 - m^2} \qquad (2.7)$$

in the ordinary $\Lambda \geq m$ region (we will see below that only the $\Lambda \geq m$ branch is compatible with both the observed pion decay constant and the pion electromagnetic mass shift).

The theory describes four (one isoscalar and three isovector) scalar and four pseudoscalar bound state modes (2.4) with masses determined by the poles in their effective propagators†

$$D_{\vec{\pi}}(p^2) = \frac{i(G_1 + G_2)}{1 - (G_1 + G_2)\Pi_{\pi}(p^2)} = \frac{-i\,g_{\pi qq}^2}{(p^2 + i\epsilon)\,F_{\pi}(p^2)}$$

*) The "Λ" on the (diverging) integral symbolizes some kind of cut–off procedure which is constrained to respect both vector and axial vector Ward identities, see below.

†) The explicit structure of the propagators will be discussed further below, in terms of the polarization insertions $\Pi(p^2)$ and of the pion electromagnetic form factor $F_{\pi}(p^2)$; here we are only interested in the *position* of the time–like poles of $D(p^2)$.

$$D_{\eta'}(p^2) = \frac{i(G_1 - G_2)}{1 - (G_1 - G_2)\Pi_\pi(p^2)} = \frac{-ig^2_{\pi qq}}{(p^2+i\epsilon)\,F_\pi(p^2) - m^2_{tH}}$$

$$D_{\sigma_0}(p^2) = \frac{i(G_1 + G_2)}{1 - (G_1 + G_2)\Pi_\sigma(p^2)} = \frac{-i\,g^2_{\pi qq}}{(p^2 - m^2 + i\epsilon)F_\pi(p^2)} \qquad (2.8)$$

$$D_{\vec{\sigma}_1}(p^2) = \frac{i(G_1 - G_2)}{1 - (G_1 - G_2)\Pi_\sigma(p^2)} = \frac{-i\,g^2_{\pi qq}}{(p^2 - 4m^2 + i\epsilon)F_\pi(p^2) - m^2_{tH}}$$

with $m^2_{tH} \equiv \frac{2\ g^2_{\pi qq} G_2}{G_1^2 - G_2^2}$ for $G_1 \neq G_2$. Note that $(\pi^0 - \eta')$ mixing occurs only in the unequal mass mode. Then, in the limit $G_1 \to G_2$ the simplest NJL model is recovered, the masses of the η' and of the $\vec{\sigma}_1$ go to infinity and thus those modes completely decouple from the theory. Note that the three pionic Goldstone modes are strongly bound ($E_B = 2m$) while the scalar σ_0 has a "mass" of $m_{\sigma_0} = 2m$ and is extremely weakly "bound" (relativistic contact of quark and antiquark). The sigma mesonic mode σ_0 should *not* be identified with the lowest mass scalar–meson resonance $f_0(975)$, but rather be treated as an effective degree of freedom which parameterizes the $q\bar{q}$ interaction in the I = J = 0 channel.

There is another interesting limit, $G_2 \to 0$; in this limit the mass of the η' goes to zero (it becomes the fourth Goldstone mode) and $m_{\vec{\sigma}_1} \to m_{\sigma_0}$, as expected. It might be tempting to fit $G_{1,2}$ to the observed [7] $m_{\eta'} = 958$ MeV, $m_{\vec{\sigma}} = m_{a_0} = 983$ MeV. This, however, does not make sense within a two–flavour model, due to the substantial $s\bar{s}$ component of the η'. Without trying to address the problems associated with implementing the $2N_f$ – Fermion interaction of the 't Hooft term†) in $N_F > 2$ models [8] we show schematically in Fig. 2 how the η' (and η) mass might be generated.

Since the NJL Lagrangian contains four–Fermion contact interactions, it is not renormalizable in 3+1 dimensions. The problem of regularizing loop integrals in the NJL

†) In the Hartree–Fock approximation this term is entirely responsible for flavour mixing.

model has been extensively discussed in the literature (for a recent overview see ref. [8]). Any cut–off procedure introduces one new arbitrary constant Λ, so that the simplest NJL model has two parameters G and Λ. Common to any reliable cut–off procedure is also that it fulfills both vector and axial–vector Ward identities. Historically, the Pauli–Villars regularization scheme [9] was the first to fulfill this requirement. A more recent one is the dimensional regularization scheme [10].

In order to gain predictive power, the two parameters (G,Λ) have to be expressed in terms of two independent observables. The standard choice has been the precisely measured pion weak decay constant f_π, and the quark scalar condensate $<\bar{\psi}\psi>_0$ or the constituent quark mass m (the two are simply related in the Hartree approximation). Neither m nor $<\bar{\psi}\psi>_0$ is an observable, so that it has recently been suggested to select the pion electromagnetic mass shift as the second observable instead [11]. It is well–known [12] that for fixed values of f_π, the gap equation has two different solutions m(Λ) for Λ above the critical value $\Lambda_c \sim 720$ MeV. These two solutions are characterized by m > Λ ("high–mass" branch, appropriate to the original, Fermi–Yang spirit, formulation of the model) and m < Λ ("low–mass" branch, corresponding to the modern quark–model interpretation of pseudo–scalar mesons). It turns out that only the (m <Λ) – branch can reproduce *both* the observed f_π *and* the electromagnetic mass shift [11,13], thus resolving the previous ambiguity in the gap equation.

III Pion observables

We have seen in the previous section that the NJL model reproduces in an approximate way the observed mass pattern among scalar and pseudoscalar mesons: almost zero–mass pseudoscalar–isovector mesons and a much heavier scalar–isoscalar meson (possibly degenerate with the scalar–isovector mesons, depending on the ration G_1/G_2). This is in line with valence quark models of mesons, where the pseudoscalar $q\bar{q}$

configurations naturally form the lowest states for which the q and $\bar{q}$ are in a relative s–state with spins coupled to total spin zero, and the resultant parity of these pairs is negative due to opposite intrinsic parities for Fermions and Anti–Fermions, a consequence of the P–invariance of the Dirac equation.

In the absence of any current quark mass there would be 35 massless Goldstone bosons associated with the spontaneous breaking of the $SU(N_f)_L \otimes SU(N_f)_R$ chiral symmetry ($N_f = 6$ in the Standard Model). It was noted already by Nambu [4]. more than thirty years ago, that the three pions are the most natural candidates for massless Goldstone bosons associated with the spontaneous breaking of $SU(2)_2 \times SU(2)_R$: only a very small current quark mass ($\sim$ 5 MeV) is necessary to endow the pion with its observed mass, π^o (135). The reason is that $m_\pi \sim \sqrt{m_q}$, hence it rises sharply above its chiral limit value for moderately increasing quark masses m_q. Due to the pion's extreme proximity to the chiral limit we discuss this first in subsection A and leave the discussion of the small non–chiral corrections for B.

(A) Chiral limit

Most of the pion observables can be expressed in terms of a (diverging) loop–integral

$$I(q^2) = \int^{\Lambda} \frac{d^4p}{(2\pi)^4} \frac{1}{(p^2-m^2)\,((p+q)^2-m^2)} \qquad (3.1)$$

$$= I(0) - \frac{i}{(4\pi)^2} \int_0^1 dz\, \ell n\, (1 - \frac{q^2}{m^2} z(1-z))$$

where the divergent piece I(0) has been isolated in the last equation.

A.1 Strong + Weak observables

Within the H + RPA scheme, Γ_π can be expressed as (see Fig. 3a)

$$\Gamma_\pi^2 = -\, 4N_c\, i\, m^2\, I(0) \qquad (3.2)$$

where m solves the gap equation

$$m = \Sigma_H = 16\, i\, m\, G N_c \int^{\Lambda} \frac{d^4p}{(2\pi)^4} \frac{1}{p^2-m^2} \qquad (3.3)$$

The reason for the appearance of the Goldstone mode in (H. + RPA) is the relation between the quark self–energy Σ_H and the pion polarization function Π_π (see fig. 1d) that one obtains in this approximation

$$\Pi_\pi(q^2) = \frac{\Sigma_H}{2mG} + \frac{q^2\, F_\pi(q^2)}{g^2{}_{\pi qq}} \qquad (3.4)$$

$$\text{where} \qquad g^2_{\pi qq} = \left[\frac{\partial \Pi_\pi(q^2)}{\partial q^2} \right]^{-1}_{q^2=0} \qquad (3.5)$$

and $F_\pi(q^2) = I(q^2)/I(0)$ is the electromagnetic form factor to one–loop order, see fig. 4. The effective pion propagator (2.8), given by the sum of proper polarization diagrams as in Fig. (1c,d) is

$$D_\pi(q^2) = \frac{-\, i\, g^2_{\pi qq}}{(q^2 + i\,\epsilon) F_\pi(q^2)} \qquad (3.6)$$

and propagates a Goldstone mode.

A low $-q^2$ expansion of $D_\pi(q^2)$ using $F_\pi(q^2) = 1 + \frac{1}{6} q^2 <r_\pi^2> + O(q^4)$, yields

$$D_\pi(q^2) = \frac{-ig^2_{\pi qq}}{q^2} + i \frac{g^2_{\pi qq}}{6} <r_\pi^2> + O(q^2) \tag{3.7}$$

which can be directly compared with the corresponding expansion coefficients as obtained in chiral perturbation theory (CHPTH) [14,15] for the two–point function of pseudoscalar quark currents, with the result

$$<r_\pi^2> = 24 \frac{2L_8 - H_2}{f_\pi^2} \tag{3.8}$$

where L_8 and H_2 are one of the low– and high–energy parameters describing the general effective Lagrangian density of order q^4 [15]. Using the value $L_8 = (0.9 \pm 0.3) \times 10^{-3}$ obtained in the analysis of ref [14] and the chiral limit result for $<r_\pi^2>$ (see eq. (3.19) below) our result for H_2 is $H_2 = 2L_8 - \frac{1}{32\pi^2} = (-1.4 \pm 0.6) \times 10^{-3}$. This compares well with the values obtained in refs. [14,16].

From Fig. 1d it is clear that $\Pi_\pi \sim N_c$, this implies via (3.5)

$$g_{\pi qq} \sim N_c^{-\frac{1}{2}} \tag{3.9}$$

as expected from QCD. This dependence on N_c will be important for our discussion of the next–to–leading order $O(1/N_c)$ corrections to the NJL model, see below. This characteristic QCD N_c–dependence of $g_{\pi qq}$ in the pion propagator and the fact that each quark loop introduces another factor N_c demonstrates that an expansion of classes of Feynman diagrams in terms of meson–quark vertices (in analogy to the photon quark vertex in QED which introduces a factor $\sqrt{\alpha}$) does not make sense. Diagrams with *one* more fermion loop *and* one more internal meson do not change the diagram's order in N_c,

see our discussion below.

Using the quark axial Ward identities it is straight–forward to derive the Goldberger– Treiman (GT) relation

$$f_\pi g_{\pi qq} = m, \tag{3.10}$$

i.e. $g_A^{quark} = 1$. We will see that g_A^{quark} remains 1 even after inclusion of $O(\frac{1}{N_c})$ corrections; the axial charge is only renormalized by $O(N_c^{-2})$ contributions.

The quark condensate density

$$<\bar\psi\psi>_0 \equiv <0|\bar\psi(x)\psi(x)|0>$$

in the *interacting* vacuum state $|0>$ does not vanish, as a result of the spontaneous dynamical breaking of chiral symmetry,

$$m = m_0 - 2G <\bar\psi\psi>_0 \tag{3.11}$$

with $m_0 = 0$ in the chiral limit considered here. This result concludes the "strong + weak" pion observables; we now turn to the "strong + electromagnetic" pionic observables.

A.2 Electromagnetic observales

It turns out that the NJL model is particularly sensitive to it's parameters (G,Λ) when it comes to comparisons with electromagnetic amplitudes involving the RPA–pion field.

A.2.1 Decay width of the neutral pion

In the chiral limit the NJL model reproduces the observed axial anomaly in the $\pi^0 \to \gamma\gamma$ decay amplitude [7] see Fig. 3b,

$$\frac{\Gamma^{Exp}_{\pi^0 \to \gamma\gamma}}{m^3_{\pi^0}} = \frac{7.8\ \ (5)\ \text{eV}}{m^3_{\pi^0}} = 3.2(2) \times 10^{-6}\ \text{GeV}^{-2} \tag{3.12}$$

in the form ($f_\pi = 92.4(2)$ MeV, including $O(\alpha)$ corrections [17], and $\alpha \equiv 1/137$):

$$\frac{\Gamma^{NJL}_{\pi^0 \to \gamma\gamma}}{m^3_{\pi^0}} = \frac{\alpha^2}{64\pi^3 f^2_\pi}\, h\,(\Lambda/m)$$

$$= 3.14 \times 10^{-6}\ \text{GeV}^{-2} \times h\,(\frac{\Lambda}{m}) \tag{3.13}$$

where h (Λ/m) is a strongly varying function of Λ/m between 0 and 2 [12,18]. A comparison of (3.12) and (3.13) suggests values of Λ and m such that $h(\Lambda/m) \approx 1$. Relatively small values for the constituent quark mass m are preferred: for $m \lesssim 250$ MeV and Λ/m of order 4 one obtains values in (3.13) which are within 10% of the empirical values, eq. (3.12). Note that h $(\Lambda/m) \equiv 1$ in (3.13) represents the model–independent Adler–Bell–Jackiw anomaly (as derived, for example, in the linear sigma model [19]). The analysis of $\Gamma_{\pi^0 \to \gamma\gamma}$ alone shows that the NJL model in two different regions of (Λ/m) corresponds to different realizations of the sigma model in lowest order of N_c : the limit $(\Lambda/m) \to 0$ recovers the non–linear sigma model (no σ–meson and no quarks), while the limit $(\frac{\Lambda}{m}) \to \infty$ gives $g_{\pi qq} \to 0$ and recovers the linear sigma model, in this order.

A.2.2 Pion Polarisabilities

If the Goldstone pion is embedded in an electromagnetic field $(\vec{E},\vec{B})$ its mass varies quadratically with the applied field for small field–strength†

$$\Delta m_\pi = -\frac{1}{2}\,\alpha_\pi\,\vec{E}^2 \ \text{ for an electric field}$$

$$\Delta m_\pi = \frac{1}{2}\,\beta_\pi\,\vec{B}^2 \ \text{ for a magnetic field} \tag{3.14}$$

The NJL model gives [8]

$$\frac{\alpha_{\pi_0}}{m_{\pi_0}} = -\frac{\beta_{\pi_0}}{m_{\pi_0}} = \frac{5}{96}\,\frac{e^2}{\pi^4 f^4_\pi}\,(1 - \frac{2\pi^2 f^2_\pi}{3m^2})$$

$$= 8.8 \times 10^{-5}\ \text{fm}^4 \tag{3.15}$$

and for the charged pions [21] one obtains

$$\frac{\alpha_{\pi^\pm}}{m_{\pi^\pm}} \simeq (15 - 18) \times 10^{-4}\ \text{fm}^4$$

$$\frac{\beta_{\pi^\pm}}{m_{\pi^\pm}} \simeq -(15 - 17) \times 10^{-4}\ \text{fm}^4\,. \tag{3.16}$$

Experimentally, the polarisability for charged pions is poorly known in the combination [22].

$$\frac{\alpha_{\pi^\pm} + \beta_{\pi^\pm}}{m_{\pi^\pm}} = (2.0 \pm 7.8) \times 10^{-4}\ \text{fm}^4 \tag{3.17}$$

---

† This expression is only correct up to relativistic effects; a complete analysis relates α_π, β_π to the first two invariant form factors of the pion Compton scattering amplitude [20].

while nothing is known about α_{π^0}, β_{π^0}.

A.2.3 Pion Form Factors and Electromagnetic Mass Shift

The pion has two form factors, one ($\Gamma_\pi(q^2)$) a scalar and the other ($F_\pi(q^2)$) a vector. The scalar form factor $\Gamma_\pi(q^2)$ does not have a chiral limit and will, therefore, be discussed in section B, where non–chiral effects are dealt with. The isovector form factor $F_\pi(q^2)$ has been calculated in the NJL model to one–loop order (Fig. 4) by many authors [8,11–13]. In the chiral limit a closed form result is obtained [8]. In the space–like region $q^2 = -Q^2 \leq 0$ one finds for small η

$$F_\pi(q^2) = 1 + \beta\,(1 - \sqrt{1+\eta^{-1}}\,\log\,(\sqrt{\eta} + \sqrt{1+\eta})) \tag{3.18}$$

where $\eta \equiv Q^2/4m^2$ and $\beta = \frac{3}{2\pi^2}\left[\frac{\partial\Pi_\pi(q^2)}{\partial q^2}\right]^{-1}_{q^2=0} = \frac{3m^2}{2\pi^2 f_\pi^2}$. In the time–like region $F_\pi(q^2)$ can be obtained from the once–subtracted dispersion relation

$$\mathrm{Re}\,F_\pi(q^2) = 1 + \frac{q^2}{\pi}\int_{4m^2}^{\infty} dt\,\frac{\mathrm{Im}\;F_\pi(t)}{t(t-q^2+i\epsilon)} \tag{3.19}$$

with $\mathrm{Im}\,F_\pi(q^2) = \theta(q^2-4m^2)\,\beta\,\frac{\pi}{2}\sqrt{1-4m^2/q^2}$.

We return to the explicit form of $F_\pi(q^2)$ in the different kinematical regions in Section B ($m_\pi \neq 0$). Associated with $F_\pi(q^2)$ is a pionic charge distribution, defined in the Breit–frame (where $q_o = 0$ and $q^2 = -\vec{q}^2$),

$$\rho_\pi(\vec{r}) = \int \frac{d^3q}{(2\pi)^3}\,e^{i\vec{q}\cdot\vec{r}}\,F_\pi(\vec{q}^2) \tag{3.20}$$

Using the form (3.18) and eq (3.19) one finds

$$\rho_\pi(\vec{r}) = \delta^{(3)}(\vec{r})\,(1 - \frac{1}{\pi}\int_{4m^2}^{\infty}\frac{dt}{t}\,\mathrm{Im}\,F_m(t)) + \frac{\beta m}{2\pi r^2}\,K_1(2mr) \tag{3.21}$$

where K_1 is a modified cylindrical Bessel function. One can verify that this $\rho_\pi(\vec{r})$ is properly normalized to the total pionic charge consistent with $F_\pi(0) = 1$. Several remarks concerning eq (3.18) – (3.20) are in order :

(i) The dispersive integral in eq. (3.19) starts at the $q\bar{q}$ threshold $4m^2$, in direct conflict with confinement, as expected.

(ii) The calculated slope of the NJL $F_\pi(q^2)$ at the origin reproduces the (model–independent) chiral limit result [23] for the pion charge radius squared to one–fermion–loop order,

$$\langle r_\pi^2\rangle^{\mathrm{NJL}} = \langle r_\pi^2\rangle^{\mathrm{chiral}} = \frac{3}{4\pi^2 f_\pi^2} = (0.59\mathrm{fm})^2 \tag{3.22}$$

that compares well with the measured value [24]

$$\langle r_\pi^2\rangle^{\mathrm{Exp}} = (0.657(12)\mathrm{fm})^2\,. \tag{3.23}$$

This agreement with the low $-q^2$ data is striking (see also Fig. 7 of ref 11b), given the apparent limitations of this model.

(iii) The imaginary part of $F_\pi(q^2)$ converges to a constant for $q^2 \to \infty$ in conflict with confinement; this large $-q^2$ behaviour of $F_\pi(q^2)$ is reflected in the pathological behaviour of $\rho_\pi(r)$, eq. (3.21), near the origin. In short : the non–renormalisable NJL model can only be applied to the low $-q^2$ region (equivalent to the medium–to–long range r–region).

For $r \geq 0.25$ fm the NJL $\rho_\pi(r)$ compares well with the vector meson dominance (VMD) result

$$\rho_\pi^{\mathrm{VMD}}(r) = \frac{m_\rho^2}{4\pi r^2}\,e^{-m_\rho r} \tag{3.24}$$

derived from the VMD monopole fit

$$F_\pi^{VMD}(q^2) = \frac{m_\rho^2}{m_\rho^2 - q^2 - i m_\rho \Gamma_\rho \theta(q^2 - 4m_\pi^2)} \tag{3.25}$$

with $m_\rho \approx 770$ MeV, $\Gamma_\rho \simeq 150$ MeV. One notes (Fig. 7 of [11b] that the space–like region (in particular the pion radius) is fairly well reproduced for $-5 < \frac{q^2}{4m^2} < +1$ whereas the time–like region fails to reproduce the observed form factor in the ρ–resonance region. However, the model reproduces fairly well the *integrated* strength, measured by $\int_{4m^2}^{\infty} dt\ \mathrm{Im}\ F_\pi(t)/t^2$, of the time–like form factor, which is equal to $\frac{\pi}{6} \langle r_\pi^2 \rangle$.

We now turn to the calculation of the isospin–violating mass difference between the charged and neutral pions. This difference is measured as [25]

$$\Delta m_\pi^2 \equiv m_{\pi^\pm}^2 - m_{\pi^0}^2 = (35.577(2)\ \mathrm{MeV})^2 \tag{3.26}$$

The origin of this mass difference is predominantly electromagnetic. The contribution from the up–down current quark mass difference $(m_d^0 - m_u^0)$ is only 2% of the measured mass difference and will be discussed in Section B. This allows to work in the chiral limit without making a bad mistake. In order to understand the sign of the mass shift in eq. (3.26) (note that this sign is *negative* for the nucleon, kaon and B–meson systems [7]) one considers the Coulomb energy of two charged particles, in our case a quark and an anti–quark, that form a bound pair due to the strong interaction,

$$E_C = \frac{e^2}{2} \int\int d^3r\, d^3r' \frac{\rho_\pi(\vec{r})\rho_\pi(\vec{r}')}{4\pi|\vec{r} - \vec{r}'|} = \frac{e^2}{2} \int \frac{d^3q}{(2\pi)^3} \frac{F_\pi^2(-\vec{q}^2)}{\vec{q}^2} \tag{3.27}$$

This energy is clearly positive for two charges of equal sign (as in $\pi^\pm$), and negative for two oppositely charged particles (as in π^0). This explains the observed positive sign in (3.26). Equation (3.27) indicates that the Coulomb energy has something to do with an integral over the electromagnetic form factor $F_\pi(q^2)$ of the bound state. The fully $F_\pi(q^2)$ covariant field theoretic analogue of (3.27) is

$$E_C = \frac{e^2}{2} \int\int d^4x\, d^4y \langle \pi |\, T^*(j^\mu(x) j^\nu(y))\, | \pi \rangle D_{\mu\nu}(x-y) \tag{3.28}$$

where $j^\mu(x)$ is the electromagnetic current operator, T^* denotes the covariant time ordered product including "Schwinger" terms, and $D_{\mu\nu}$ is the photon propagator. Using current algebra techniques and dominance of the single–pion intermediate state, see fig. 5, eq (3.28) can be brought into the momentum – space form [26]

$$\Delta m_\pi^2 = 3e^2 i \int \frac{d^4q}{(2\pi)^4} \frac{F_\pi^2(q^2)}{q^2 + i\epsilon} \tag{3.29}$$

or, more generally [27],

$$\Delta m_\pi^2 = 3e^2 i \int \frac{d^4q}{(2\pi)^4} \frac{1}{q^2 + i\epsilon} \frac{q^2}{2f_\pi^2} (\Pi_V^{(1)}(q^2) - \Pi_A^{(1)}(q^2)) \tag{3.30}$$

with $\Pi_{V,A}^{(1)}$ the vector and axial vector spectral functions.

After a Wick–rotation of q^μ in (3.29) one finds

$$\Delta m_\pi^2 = \frac{3\alpha}{4\pi} \int_0^\infty dQ^2\, F_\pi^2(-Q^2) \tag{3.29'}$$

and a corresponding expression for (3.30). Note that Δm_π^2 only depends on the behaviour of the form factor/spectral functions in the *space*–like region. Their resonant content

enters, therefore, not directly but rather in a dispersive way (see eq. (3.19)) which tends to average out details of those resonances (ρ,ρ',ρ'', ..., a_1, a_1', ... , π, π', ...) .

Saturating the spectral functions with the ρ–, π– and a_1 – poles together with the Weinberg sum rules which relate f_π, g_A and g_ρ and $m_{a_1} = \sqrt{2}\, m_\rho$, one obtains [27a]

$$\Delta m_\pi^2 = \frac{\alpha}{\pi}\frac{3}{2}\, m_\rho^2 \log 2 = (37.8\ \mathrm{MeV})^2$$

whereas the VMD ansatz (3.25) in (3.29) yields

$$\Delta m_\pi^2 = \frac{\alpha}{\pi}\frac{3}{4}\, m_\rho^2 = (32.1\ \mathrm{MeV})^2$$

A recent calculation [14] splits the q^2– integration in (3.30) into long distance ($0 \leq -q^2 \leq \mu^2$) and short distance ($-q^2 > \mu^2$) contributions. The long distance (i.e. low $-q^2$ region) can be fixed in principle (for $\mu^2 < m_\rho^2$) by chiral perturbation theory (CHPTH) [15] and the short distance part by using the operator product expansion [28]

$$\Pi_V^{(1)}(q^2) - \Pi_A^{(1)}(q^2) = -\frac{1}{Q^6}\,\frac{9\pi^2}{2}\,\frac{\alpha_s(Q^2)}{\pi}\,(<\bar\psi\psi(Q^2)>_0)^2 \qquad (3.31)$$

with $Q^2 = -q^2$ the euclidean 4–momentum. Unfortunately (3.31) can not be applied for $\mu^2 < m_\rho^2 < 1$ GeV^2 so that one has to resort here to long distance models that allow $\mu^2 \gtrsim 1$ GeV^2. Such a model is our two – flavour NJL model. The analogous set of gauge invariant Feynman diagrams to Fig. 5 (lowest order in α) is given in Fig. 6, after minimal substitution $i\partial^\mu\gamma_\mu \to i\partial^\mu\gamma_\mu - e_q A^\mu\gamma_\mu$ in the chiral NJL Lagrangian (2.1). Carrying out the calculation in terms of the set of $O(\alpha)$ Feynman diagrams in Fig. 6 that obey gauge invariance, as well as the vector Ward identities, one finds that only the charged pion is shifted in mass. The neutral pion remains a Goldstone particle of zero mass in agreement with Dashen's theorem [29]. This is the result of an *exact* cancellation between

contributions from the repulsive tad–pole Fig. 5b1, 6b1 and from the negative Coulomb interaction terms Fig. 6b 2–4 (Fig. 6a vanishes for π^0). The resulting mass shift can be expressed in terms of $F_\pi(q^2)$:

$$\Delta m_\pi^2 = 3e^2 i \int \frac{d^4q}{(2\pi)^4}\,\frac{F_\pi(q^2)}{q^2 + i\epsilon} \qquad (3.32)$$

This formula differs from eq (3.29) by one power of $F_\pi(q^2)$ because the full, off–shell behaviour of $F_\pi(q^2)$ has been incorporated in (3.32).

Inserting $F_\pi^{NJL}(q^2)$, eq (3.18), into eq (3.32) one finds a closed form expression for Δm_π^2 in terms of f_π, m and Λ

$$\Delta m_\pi^2 = \frac{3\alpha}{\pi} m^2\,[\,(1+\frac{3}{2}\beta)\,x^2 - \frac{1}{2}\beta\,\sinh^{-1}x\,(\sinh^{-1}x + 2\,x\,\sqrt{1+x^2})\,] \qquad (3.33)$$

where β as in eq (3.18) and $x = \Lambda_E/m$ with the euclidean cut–off Λ_E being related to the Pauli–Villars (PV) cut–off (which respects the vector and axial–vector Ward identities) Λ_{PV} by [11]

$$\Lambda_{PV}^2 = (2\log 2)^{-1}\,\Lambda_E^2 \qquad (3.34)$$

We note here that it is important to regulate in the PV scheme, the euclidean cut–off scheme does not respect Ward identities but is a very convenient scheme and, fortunately, numerically very close to the PV scheme if one identifies the relevant cut–off Λ_E from eq. (3.34). Both $(\Delta m_\pi^2)^{\frac{1}{2}}$ and m display a strong (Λ/m) dependence while $<\bar\psi\psi>_0$ is insensitive to (Λ/m). If one fixes the NJL parameters by comparison to f_π and Δm_π^2, instead of the previously used $<\bar\psi\psi>_0$, one obtains [11]

$$\Lambda_{PV} = 924 \text{ MeV } (\Lambda_E = 1088 \text{ MeV}) \qquad (3.35)$$

The value (3.35) leads to m = 225 MeV and $<\bar{\psi}\psi>_0 = -(260 \text{ MeV})^3$. Such relatively small values for m are also favoured by a comparison to $\Gamma_{\pi^0 \to \gamma\gamma'}$ see section (A.2.1). One must note here, however, that non–chiral corrections will change these values. We will see in section B that a refitting of the quark mass m and cut–off Λ to give the correct experimental mass splitting leads to m = 251 MeV and $\Lambda_E = 945$ MeV. Also the meson cloud corrections to the (H + RPA) scheme, discussed below, tend to increase the constituent quark mass further.

The result (3.33) was obtained by cutting off the (euclidean) 4–momentum of the photon, $Q^2 = -q^2 \leq \Lambda_Q^2$, after a Wick rotation of the integral in (3.32). This cut–off is not a new parameter but is restricted by the maximum momentum transfer $\Lambda_Q = 2\Lambda_E$ that the NJL model can support, where Λ_E is the NJL covariant cut–off on the quark (euclidean) phase space. The NJL pion form factor (3.18) if extrapolated to larger η–values has a zero at $-q^2 \approx 3$ (GeV)^2 and tends logarithmically to $-\infty$ for $-q^2 \to \infty$. This means that the Q^2–integration region in (3. 32) includes the zero of $F_\pi(-Q^2)$ and the region beyond, where $F_\pi(-Q^2)$ is negative. This region of Q^2 is, of course, outside the applicability of (3.18); one should use the NJL $F_\pi(q^2)$ only in the long distance regime $-q^2 \leq \mu^2 \approx 1$ GeV^2 and use eq (3.31) in (3.30) for the short distance ($-q^2 > \mu^2 \approx 1$ GeV^2) where the NJL does not properly describe the pion, recall our discussion of $\rho_\pi(r)$ after eq (3.23).

If one uses a simplified running coupling constant ($\mu \approx \Lambda_{QCD}$ assumed) [28,30]

$$\frac{\alpha_s(Q^2)}{\pi} = \frac{6}{33 \log(\frac{Q}{\mu})} \qquad (3.36a)$$

and scalar quark condensate

$$<\bar{\psi}\psi(Q^2)_0 = <\bar{\psi}\psi>_0 (\log(\frac{Q}{\mu}))^{9/22} \qquad (3.36b)$$

with $<\bar{\psi}\psi>_0 \approx -(260 \text{ MeV})^3$ one finds indeed that the matching parameter $\mu \approx 1$ GeV reproduces the empirical Δm_π^2. This agrees with an independent investigation in the "extended" NJL model [14].

A.3 $O(\frac{1}{N_c})$ corrections to the NJL model

A particularly important and long–standing issue has been the construction of the subleading approximation, beyond the Hartree–Fock + RPA, that preserves chiral symmetry. The Fock terms, Fig. 1b, are the first $O(1/N_c)$ correction. They are, however, "trivial" in the sense that they can be evaluated by using a Fierz–rearranged interaction Lagrangian, and they do not involve any modification of RPA in the two–body Schwinger Dyson equation. Here we leave the Fock terms out and stay in the Hartree approximation. Note that this is self–consistent because the Ward identities are *separately* satisfied by the Fock terms.

The similarity of the NJL model to the renormalizable linear sigma model in leading order of $1/N_c$ guides us to find a self–consistent set of Feynman diagrams which go beyond the (H+RPA) scheme. In the sigma model the higher–order one–meson loop diagrams, Fig. 7, have been shown [31] to respect Goldstone's theorem. The one–meson loop diagrams of Fig. 7 can easily be calculated (and be shown to vanish in the sum) in the U(1) symmetric sigma–model Lagrangian

$$\mathscr{L}(\hat{\sigma},\pi) = \frac{1}{2}((\partial_\mu\hat{\sigma})^2 + (\partial_\mu\pi)^2) + \frac{\mu^2}{2}(\hat{\sigma}^2 + \pi^2) + \frac{\lambda}{4}(\hat{\sigma}^2 + \pi^2)^2$$

which is spontaneously broken by choosing the vacuum such that only the "physical" σ field

$$\sigma = \hat{\sigma} - <\hat{\sigma}>_0$$

has a vanishing vacuum expectation value, with the new Lagrangian

$$\mathcal{L}(\sigma,\pi) = \frac{1}{2}\left((\partial_\mu\sigma)^2 + (\partial_\mu\pi)^2\right) - \mu^2\,\sigma^2 - \lambda < \bar{\sigma} >_0 \sigma(\sigma^2+\pi^2) - \frac{\lambda}{4}(\sigma^2+\pi^2)^2 \qquad (3.37)$$

which has a massless field π and a massive $(2\mu^2)$ field σ interacting through $\sigma\pi\pi$, $\sigma\sigma\sigma$, $\sigma\sigma\pi\pi$, $\sigma\sigma\sigma\sigma$ and $\pi\pi\pi\pi$ vertices. The contributions to the pions self energy $\Sigma(p^2)$ coming from the 5 diagrams in Fig. 8 sum up to zero [31]

$$\Sigma(0) = \Sigma^a(0) + \Sigma^{b1}(0) + \Sigma^{b2}(0) + \Sigma^{b3}(0) + \Sigma^{b4}(0) \equiv 0 \qquad (3.38)$$

where $\Sigma^a(0) = 2\lambda\,(I^{(0)}(2\mu^2) - I^{(0)}(0))$

$\Sigma^{b1}(0) = -\lambda\, I^{(0)}(0)$

$\Sigma^{b2}(0) = -3\lambda\, I^{(0)}(2\mu^2)$

$\Sigma^{b3}(0) = 3\lambda\, I^{(0)}(0)$

$\Sigma^{b4}(0) = \lambda\, I^{(0)}(2\mu^2)$

with the quadratically diverging integral

$$I^{(0)}(z) = \int \frac{d^4p}{(2\pi)^4}\,\frac{1}{p^2 - z}$$

which, in the NJL model, is related to the scalar condensate

$$I^{(0)}_{NJL}(m^2) = -\frac{<\bar{\psi}\psi>_0}{4\,i\,m\,N_c} \qquad (3.39)$$

In the sigma model $I^{(0)}(2\mu^2)$ is essentially the tadpole diagram [31]. This little exercise

clarifies also the role of the pion–pole diagram, Fig. 7a where the product of two meson propagators under the integral (one of them massless) splits into the difference of two single propagators. This leads to the required cancellation in (3.38).

Recalling the analogy between QED sigma model diagrams, Fig. 5, and QED NJL diagrams, Fig. 6, one is led to consider the QCD diagrams in Fig. 8. Indeed, these NJL diagrams are all of the same order $0(1/N_c)$, respect all Ward identities, and the pion remains a Goldstone mode after inclusion of these "meson cloud" corrections to the (H + RPA) scheme [32]. Fig. 8a and Figs. 8b are of the same order in N_c because the additional fermion loop in (8a) introduces an additional factor N_c which, however, cancels against the additional factor N_c^{-1} due to an additional meson exchange in Fig (8a), see also eqs (3.9), (3.6).

The cancellation leading to $\Sigma_{NJL}(0) = 0$ analogous to eq (3.38) occurs in the same way in the NJL model if one identifies the diagrams in Fig. 8 with the corresponding ones in Fig. 7. The resulting Σ^a_{NJL}, Σ^{bi}_{NJL} (i = 1,2,3,4) reduce to the ones in (3.38) in the limit $m \to \infty$, but (Λ/m) finite. This emphasizes again the similarity to the sigma model in terms of sets of Feynman diagrams classified by a given order ("one meson loop" diagrams in the sigma model have a corresponding set of $O(\frac{1}{N_c})$ diagrams in the NJL model) ; but it also shows that the NJL model gives a richer structure to the hadronic tadpole diagrams of the sigma model. It is also found that the axial quark coupling g^q_A is unrenormalized by $O(1/N_c)$ diagrams and stays at $g^q_A = 1$. This is perfectly consistent with the renormalization conditions appropriate to particles which are not elementary [33]. The additional meson loops in Fig. 8 require an additional meson–loop cut–off $\tilde{\Lambda}$. Here, again, comes in the non–renormalizability of the NJL model. This parameter $\tilde{\Lambda}$, however, has an *upper* limit (for fixed Λ)

$$\tilde{\Lambda} < 0.73\,\Lambda$$

as a result of the solubility condition of the gap equation [32]. This maximal value lies far below the zero of $F_\pi(-Q^2)$ which otherwise would introduce a space–like (tachyonic) pole into the pion and sigma propagators. One finds that m varies from its Hartree value ($\tilde{\Lambda} = 0$) m = 225 MeV up to 360 MeV at the maximal $\tilde{\Lambda} = 0.73\ \Lambda$ (for $\Lambda = \Lambda_E = 1088$ MeV). This variation is indeed of $O(1/N_c)$, as expected. Thus there seems to be a self–regulating mechanism that keeps the value of $\tilde{\Lambda}$ below the zero of $F_\pi(-Q^2)$ and provides an upper bound on the corrections to the Hartree terms. If one couples a photon field to all charged particles in the diagrams Fig. 8 one obtains meson cloud corrections to $F_\pi(q^2)$

$$F_\pi(q^2) = (1-b)\, F_\pi^{\bar{q}q}(q^2) + b\, F_\pi^{\pi\pi}(q^2) \tag{3.40}$$

where $F_\pi^{\bar{q}q}$ refers to the previous H + RPA result, eq (3.18) and $F_\pi^{\pi\pi}(q^2)$ is essentially the contribution from the final state interaction in terms of σ–meson exchange, Fig. 9. "b" in (3.40) is small (≈ 0.08) and, although the imaginary part of $F_\pi^{\pi\pi}(q^2)$ converges to zero for $q^2 \to \infty$, there is no "ρ–like" structure in the time–like region. The space–like region of $F_\pi(q^2)$ is slightly improved but still very close to the H + RPA result. In the following we want to indicate how one could, in a systematic way, obtain the next higher order diagrams. These next order loop diagrams ($1/N_c^2$ relative to the leading one–loop diagram Fig. 1a,c) are depicted in Fig. 10 (the different momentum routings and/or crossed diagrams are not shown). We have in addition the 3π– and $\sigma\sigma\pi$– intermediate states (a), the double–tadpoles (b1) and (c) and a new "tower" diagram (d) topologically similar to the second diagram in (a), and a "meson–cloud" contribution to the gap–equation (b2) which renders the quark selfenergy momentum dependent (a major obstacle). Solving the new gap equation self–consistently without new approximations is a formidable task.

Another presently unanswerable question is if the set of diagrams shown under

Fig. 10 is indeed *complete* within the NJL model. The path integral approach to QCD in the light–front [34], though promising, is unable in its present form to settle this question, because it involves several *approximations* as well (lower dimensions, saddle–point method etc).

(B) Non–chiral corrections

We consider now the case $m_0 \neq 0$ in $\mathcal{L}_{NJL}$, eq (2.2), so that chiral symmetry is now *explicitly* broken and the pion acquires a mass given by the model–independent, current algebraic formula [29]

$$m^2(\pi_a) = \frac{1}{f_{\pi_a}^2} < 0\ |[Q_a^{5+}, [Q_a^5,\ \mathcal{L}_{nc}(0)]]|\ 0 > \tag{3.41}$$

This formula describes the lowest order correction to the zero pion mass as a consequence of chiral symmetry breaking terms $\mathcal{L}_{nc}(0)$ in the QCD Lagrangian and is not valid in a situation where the chiral symmetry is not exact to begin with. Inserting $\mathcal{L}_{nc}$ from eq (2.2) into (3.41) one finds the model–independent Gell–Mann–Oakes–Renner (GMOR) relations

$$m^2_{mech}(\pi^\pm) = m^2(\pi^0) = -\frac{1}{f_\pi^2}[\, m_u^0 < 0|\bar{u}u|0 > + m_d^0 < 0|\bar{d}d|0 >\,]$$

$$m^2_{mech}(K^\pm) = -\frac{1}{f_K^2}[\, m_u^0 < 0|\bar{u}u|0 > + m_s^0 < 0|\bar{s}s|0 >\,] \tag{3.42}$$

$$m^2_{mech}(K^0) = -\frac{1}{f_K^2}[\, m_d^0 < 0|\bar{d}d|0 > + m_s^0 < 0|\bar{s}s|0 >\,]$$

between the pseudoscalar and current quark masses. It demands substantial quark scalar condensates even in the chiral limit, thus implying a highly non–perturbative ground state of QCD.

If one applies the $\mathscr{L}_{EM}$, on which eq (3.28) is based, to eq (3.41) one obtains in the chiral limit Dashen's theorem

$$m^2_{EM}(\pi^o) = m^2_{EM}(K^o) = m^2_{EM}(\eta) = 0$$
$$m^2_{EM}(\pi^\pm) = m^2_{EM}(K^\pm) \tag{3.43}$$

where m^2_{EM} is the electromagnetic mass squared of the pseudoscalar meson. If one now adds this EM to the mechanical masses $m^2_{mech}(\pi)$ that appear in the GMOR relations, and if one assumes $f_\pi = f_K$ and $< \bar{u}u >_o = < \bar{d}d >_o = < \bar{s}s >_o$, then one can use the empirically observed pion and kaon masses to extract the following two current quark mass ratios:

$$\frac{m_d^o}{m_u^o} = \frac{m^2(\pi^\pm) - m^2(K^\pm) + m^2(K^o)}{2m^2(\pi^o) - m^2(\pi^\pm) + m^2(K^\pm) - m^2(K^o)} = 1.8$$
$$\frac{m^o_s}{m^q_d} = \frac{m^2(\pi^\pm) + m^2(K^\pm) - m^2(K^o)}{m^2(\pi^\pm) - m^2(K^\pm) + m^2(K^o)} = 20 \tag{3.44}$$

These are Weinberg's current quark mass ratios that are extensively used in chiral perturbation theory today. Without the above assumptions the empirical bounds are [7]

$$\frac{m_d^o}{m_u^o} = 1.4 - 4$$
$$\frac{m_s^o}{m_d^o} = 17 - 25 \tag{3.45}$$

For later use we quote here also the empirical bounds on the *individual* current quark masses [7]

$$m_d = (5\text{–}15)\ \text{MeV} \qquad m_u = (2\text{–}8)\ \text{MeV}$$
$$m_s = (100\text{–}300)\ \text{MeV} \qquad m_c = (1.3 - 1.7)\ \text{GeV} \tag{3.46}$$
$$m_b = (4.7 - 5.3)\ \text{GeV} \qquad 55\ \text{GeV} < m_t < 200\ \text{GeV}$$

These quark masses reflect the pattern of breaking of weak and electromagnetic gauge symmetries; in the present theoretical framework, the Standard Model, there is no understanding of the observed quark mass hierarchy, eq (3.46).

We return to the first equation in (3.42) and note that $m^2_{mech}(\pi^\pm)$ and $m^2_{mech}(\pi^o)$ can only differ due to a different $f^2_{\pi^\pm} \neq f^2_{\pi^o}$ in (3.42). This difference is quadratic in the quark mass difference, hence the masses squared of the charged and neutral pions are the same up to quadratic corrections,

$$(\Delta m^2_\pi)_{mech} = \Gamma_\pi (m_d - m_u)^2 \tag{3.47}$$

where Γ_π is model dependent within the range

$$1 \leq \Gamma_\pi \leq 4$$

The two–flavour NJL model considered here gives $\Gamma_\pi = 1$, and $\Gamma_\pi \approx 4$ is obtained in $(\pi^o\text{–}\eta)$ mixing schemes [35,36]. Introducing a non–vanishing current quark mass into our calculation of m and Δm^2_π, eq (3,32), requires the knowledge of the (isovector) pionic self energy $\Pi_\pi(q^2)$ at $q^2 = m^2_\pi \neq 0$. One finds

$$\Delta m_\pi^2 = -g_{\pi qq}^2 \Pi_\pi(q^2) \qquad (3.48)$$

with $\Pi_\pi(q^2) = \Pi_\pi(0) + b(\Lambda/m)q^2 + c\, q^2 \log q^2$ where b(x) is given in [13] and $c = \alpha/(2\pi g^2 \pi qq)$. The $m_\pi^2 \log m_\pi^2$ term in (3.48) is, of course, also obtained in CHPTH models [14,35,37].

If we leave (Λ_E, m) at their values (1088,225) MeV obtained in the chiral limit and calculate non–chiral corrections that way, we obtain the revised value

$$\Delta m_\pi^2 = (35.6\ \text{MeV})^2 + (12.9\ \text{MeV})^2 + (4.2\ \text{MeV})^2 = (38.1\ \text{MeV})^2 \qquad (3.49)$$

representing the pure EM, non–chiral and mechanical contributions. This value (3.49) is too large by 15%. A refitting of (Λ_E, m) leads to (945,251) MeV. Note that non–chiral effects tend to *increase* the quark mass m, a welcomed effect if such constituent quarks should ultimately be able to reproduce the nucleon mass.

Non–chiral correctional to $F_\pi^{q\bar{q}}(q^2)$ eq (3.18) are very small in both space– and time–like regions. This is not the case for $F_\pi^{\pi\pi}(q^2)$, eq (3.40) because non–chiral corrections shift the threshold $4m_\pi^2$ away from zero to the observed value below the $q\bar{q}$ threshold. The $q^2 \log q^2$ term in $F_\pi^{\pi\pi}(q^2)$ leads for $m_\pi = 0$ to an infinite slope $F_\pi'^{\pi\pi}(0)$ reflecting an infinite pion Compton wavelength. For $m_\pi \neq 0$, $F_\pi'^{\pi\pi}(0)$ becomes finite. In any event the smallness of b in (3.40) makes such effects hardly visible [38]. While chiral corrections are unimportant for $F_\pi(q^2)$ they are vital for the existence of the scalar pion form factor $\Gamma_\pi(q^2)$, which is related to the operator $(\hat{m} = \frac{1}{2}(m_u + m_d))$ $\quad \hat{m}(\bar{u}u + \bar{d}d)$ and, therefore, it is not directly measurable. However, it can be related to the scalar form factor of the nucleon and to the sigma term [39]. The current algebra result $\Gamma_\pi(0) = m_\pi^2$ is recovered in the NJL model for $(\Lambda \to \infty,\ \Lambda/m$ fixed). The slope of $\Gamma_\pi(q^2)/\Gamma_\pi(0)$ at $q^2=0$

turns out to be very sensitive to the NJL parameters. A $\pi\pi$ phase shift analysis obtains

$$< r_\pi^2 >^S = (0.77\ \text{fm})^2 \qquad (3.50)$$

compatible with the chiral perturbation theory result [15]; the NJL model one–loop result is within ~ 10% of the empirical result (3.50), if the constituent quark mass is *below* 250 MeV. Such small mass values are consistent with what one finds in fits of Δm_π^2 ; it should be noted here that the higher order diagrams *increase* m, see section 3(A.3).

In the remainder of this section we want to see if the bulk part of other pseudoscalar mass shifts could perhaps be simply related to the pion mass shift. Eq (3.44) gives a first indication of such a relation. In the absence of any current quark mass there would be 35 massless Goldstone bosons associated with the spontaneous breaking of the $SU(N_f)_L \otimes SU(N_F)_R$ chiral symmetry (N_F=6 here). The three pions are the most natural candidates for massless Goldstone bosons; the much heavier kaon $K^o(498)$ does not lend itself easily to this interpretation, let alone the even heavier pseudoscalar mesons $D^o(1864)$ and $B^o(5279)$. However, the chiral limit proves to be important also for the kaon–system in the form of Dashen's theorem (3.43): in the chiral limit (i.e. *all* $m_q \to 0$) the sum of all electromagnetic contributions to the mass of strongly bound *neutral* pseudoscalar mesons[*] (m_{π^o}, m_{K^o}, m_{D^o}, m_{B^o}, m_{T^o}) vanishes identically. In other words: the π^o–mass, in particular, stays at zero even after inclusion of dynamical EM effects; the same holds for the mass of the K^o–, D^o–, B^o–, T^o– mesons, although the chiral limit seems to be of less importance for the latter mesons. One must realize, of course, that

[*] The dominant quark–antiquark content of pseudoscalar mesons is given in Fig. 11. None of the "T mesons" have been identified to date.

Dashen's theorem refers to *strongly* bound neutral systems only, for which the EM interaction between its charged constituents is an additional (and weaker) interaction, the neutral positronium (e^+e^-) system is bound by EM interactions *only* and, therefore, does not obey Dashen's theorem.

Due to the validity of Dashen's theorem in the chiral limit it makes sense to expand all pseudoscalar meson masses around the chiral limit (i.e. in powers and logs of the current quark masses),

$$m_n^2 = A_n + \sum_q \left\{ B_n^q m_q + C_n^q m_q^2 + D_n^q m_q^2 \log m_q \right\} + \sum_{(k=3)}^{\infty} R_{n,k}^q m_q^k \qquad (3.51)$$

with n = pseudoscalar meson.

Due to Dashen's theorem we know precisely one of these coefficients

$$A_{\pi^0} = A_{K^0} = A_{D^0} = A_{B^0} = A_{T^0} = 0 \qquad (3.52)$$

Note that relation (3.52) is model independent; of course, for heavy–light mesons D,B,T the coefficients $R_{n,k}^q$ will become progressively important. A rough estimate of those terms will be given below. The logarithmic dependence on m_q is exactly in line with the CHPTH result [15,37] that is based on general chiral symmetry arguments.

For $m_q \to 0$ only the $A_{n^\pm}$ – term in $m_{n^\pm}^2$ survives, due to the Coulomb interaction of the constituents (which have a non–vanishing constituent quark mass in the chiral limit) this $A_{n^\pm}$ – term is non–vanishing and indeed positive definite [11,15,37]. This fact makes these (rather precisely measured [4]) electromagnetic mass shifts prime candidates for QCD model tests :

$$\begin{aligned}
\Delta m_\pi^2 &\equiv m_{\pi^\pm}^2 - m_{\pi^0}^2 = (35.577(2)\text{MeV})^2 \\
\Delta m_K^2 &\equiv m_{K^\pm}^2 - m_{K^0}^2 = -(63.2(2)\text{MeV})^2 \\
\Delta m_D^2 &\equiv m_{D^\pm}^2 - m_{D^0}^2 = (133(4)\text{MeV})^2 \\
\Delta m_B^2 &\equiv m_{B^\pm}^2 - m_{B^0}^2 = -(97\ \text{MeV})^2 \text{ to } +(86\ \text{MeV})^2 \\
\Delta m_T^2 &\equiv m_{T^\pm}^2 - m_{T^0}^2 = \text{not measured}
\end{aligned} \qquad (3.53)$$

In the chiral limit one obtains therefore from eq (3.51)

$$\begin{aligned}
&\Delta m_\pi^2 = A_{\pi^\pm}\ ,\ \Delta m_K^2 = A_{K^\pm}\ ,\ \Delta m_D^2 = A_{D^\pm} \\
&\Delta m_B^2 = A_{B^\pm}\ ,\ \Delta m_T^2 = A_{T^\pm}
\end{aligned} \qquad (3.54)$$

and $A_{\pi^\pm} = A_{K^\pm} = A_{D^\pm} = A_{B^\pm} = A_{T^\pm}$ (3.55)

in the chiral limit. Note that eq. (3.55) is model–independent so long as the pseudoscalar meson self–energy is based on the same chiral Lagrangian. Differences between heavy–light and light–light systems then arise due to very different current quark masses (which explicitly break the chiral symmetry of the underlying Lagrangian). In spontaneously (or: dynamically) broken chiral models different current quark masses will give rise (via a gap equation as in the NJL model or any other mass generating mechanism) to different constituent quark masses that enter the Coulomb energy part of the meson self–energy. In the chiral limit the constituent quark masses of all quark flavours are identical, hence eq. (3.55) follows. Different m_n^2 then have to arise from different B_n^q, C_n^q, D_n^q, $R_{n,k}^q$.

Let us return to the chiral limit result eq. (3.54). Obviously, eq. (3.54) is incompatible with experiment, eq (3.53), and would be completely useless if there was no information on $A_{\pi^\pm}$: it was noted already in 1961 by Nambu [4] that the $\pi(135)$ is very close to the chiral limit ($m_{u,d}$ = 5 MeV as opposed to 0). This implies that the (chiral) $A_{\pi^\pm}$, eq (3.55), must already be very close to the observed value, eq (3.53). Non–chiral corrections to m_n^2, eq (3.51), (i.e. $B_n \neq 0$, $C_n \neq 0$, $D_n \neq 0$, $R_n \neq 0$) come in two very

different varieties: (i) the (common) current quark mass $\hat{m}_q$ is non–zero and shifts the pole of the pseudoscalar meson propagator from $q^2 = 0$ to the "ur–mass" near the observed value; (ii) the current quark masses are flavour dependent and their hierarchy $m_u < m_d < m_s < m_c < m_b < m_t$ is in close analogy to hadronic mass hierarchies in simple valence quark models ($m_p < m_n$ and $m_\pi < m_K < m_D < m_B < m_T$). Due to the simple isospin structure of the pion it follows from (3.51) that

$$\Delta m_\pi^2 = A_{\pi\pm} + \hat{\Gamma}_\pi (m_d - m_u)^2 \tag{3.56}$$

with (see (3.49) and (3.47)) $\hat{\Gamma}_\pi = 1 + 9.4 = 10.4$ in the NJL model. We note, in particular, that $B_{\pi\pm} = B_{\pi^0}$ and that the relation (3.56) (i.e. no *linear* mass terms) is specific to the pion system. This quadratic dependence on the (already small) current quark masses $m_{u,d}$ demonstrates the pion's extreme proximity to the chiral limit. Model–independent estimates for $\hat{\Gamma}_\pi$ are presently unavailable, we have quoted our result in (3.56), which, however, does not include any SU(3) flavour breaking. This induces repulsion between the π^o and η levels (π^o is shifted downwards and η upwards from the "ur–mass"). The π^o–η mixing angle is small (0.01–0.02) but model dependent and its contribution to Δm_π^2 will be further modified by the mixing of π^o with the heavier η's : η' (958), η_c, η_b, η_t. For a qualitative discussion of the overall pattern of mass shifts in eq (3.45) we will ignore here the (poorly known) $\hat{\Gamma}_\pi$ term and assume

$$\Delta m_\pi^2 = A_{\pi\pm} = A_{K\pm} = A_{D\pm} = A_{B\pm} = A_{T\pm} = (35.6\ \mathrm{MeV})^2 \tag{3.57}$$

Note that eq (3.57) does not imply that all dynamical differences in heavy–light and light–light systems have been removed; such differences are still represented by the B_n^q, C_{π}^q, D_{π}^q, and R_{π}^q, terms in eq (3.51). We consider these non–chiral corrections next. For light–light pseudoscalar mesons one can represent these non–chiral corrections by the ratio of the SU(2) breaking piece to the SU(3) breaking piece of the quark mass term,

$$R = \frac{m_s - \hat{m}}{m_d - m_u} \tag{3.58}$$

In terms of the symmetry–breaking parameters ϵ_3 and ϵ_8 of the GMOR model, R stands for [35] $R = \frac{\sqrt{3}}{2} \frac{\epsilon_8}{\epsilon_3}$. Then the first order mass formula for $K^+ - K^o$ may be written, in the form (for details see ref [35])

$$\Delta m_K^2 = A_{K\pm} - (m_K^2 - m_\pi^2) \frac{1}{R} \tag{3.59}$$

and in the chiral limit $\frac{1}{R} \to 0$ (i.e. $m_s > m_d > m_u \to 0$) regaining the result eq (3.54). Our eq (3.59) represents chiral and non–chiral effects as given in eq (3.51) without the $R_{k,n}^q$ – terms, which are small for light quarks u,d,s. In addition there is a small effect (not represented by (3.59)) from the heavy quark sector due to the mixing of π^o with the heavy η's. In order to get a handle on the effects from the heavy quark mass sector for D,B,T mesons we expand these mass shifts around the first order mass formula (3.59) with constant R.

$$\begin{aligned}
\Delta m_D^2 &= A_{D\pm} + (m_{D_s}^2 - m_D^2) \frac{1}{R} + O(m_q^3) \\
\Delta m_B^2 &= A_{B\pm} - (m_{B_s}^2 - m_B^2) \frac{1}{R} + O(m_q^3) \\
\Delta m_T^2 &= A_{T\pm} + (m_{T_s}^2 - m_T^2) \frac{1}{R} + O(m_q^3)
\end{aligned} \tag{3.60}$$

where, due to Dashen's theorem, the A_n fulfill (3.57). Note that this formula (3.60) relates the *electromagnetic* mass shift to a mass–independent chiral Coulombic part A_n and to the empirical mass splitting between the heavy–strange and heavy–nonstrange mesons (in potential models this splitting reflects the *strong* interaction between flavoured

quarks); the remaining $O(m_q^3)$ terms are inaccessible by our simple approach and will be estimated in magnitude by comparison to experiments, eq (3.53). The alternating sign of the second term on the r.h.s. of eq (3.60) results from the dominant quark–antiquark assignments in Fig. 11 and from the definition of $\frac{1}{R} \sim (m_d - m_u)$, eq (3.58).

The masses of pseudoscalar mesons in eq (3.60) are experimentally known, except for m_{T_s} and m_T, so that we can write

$$\begin{aligned}
\Delta m_K^2 &= \Delta m_\pi^2 - \frac{1}{R}\, 0.226\ \text{GeV}^2 \\
\Delta m_D^2 &= \Delta m_\pi^2 + \frac{1}{R}\, 0.384\ \text{GeV}^2 + O(m_q^3) \\
\Delta m_B^2 &= \Delta m_\pi^2 - \frac{1}{R}\, (0.98 \to 1.24)\ \text{GeV}^2 + O(m_q^3) \\
\Delta m_T^2 &= \Delta m_\pi^2 + \frac{1}{R}\, (m_{T_s}^2 - m_T^2) + O(m^3{}_q)
\end{aligned} \tag{3.61}$$

Values quoted for R in the literature [8,35,37,40] are in the range

$$30 \leq R \leq 60$$

We choose R = 40 compatible with ref [35] and with the empirical mass parameters typical for $N_f = 3$ NJL models [8,40]. Then we obtain*)

$$\begin{aligned}
\Delta m_\pi^2 &= (35.6\ \text{MeV})^2 \\
\Delta m_K^2 &= -(66.2\ \text{MeV})^2 \\
\Delta m_D^2 &= (104\ \text{MeV})^2 + O(m_q^3) \\
\Delta m_B^2 &= -(152\ \text{MeV})^2 \to -(173\ \text{MeV})^2 + O(m_q^3)
\end{aligned}$$

to be compared with Eq (3.53). The $O(m_q^3)$ terms contribute ~ 20% to $(\Delta m_D^2)^{\frac{1}{2}}$ and at least 57% to $(\Delta m^2{}_B)^{\frac{1}{2}}$ emphasizing their importance for heavy–light systems. Even within the general uncertainties of $O(m_q^3)$ terms it is not very likely that they would change the sign of $\Delta m^2{}_B$ in eq (3.61). Only a better experiment for $\Delta m^2{}_B$ can decide if this mass shift is indeed *negative*, as our simple formula, eq (3.60), implies, which is based on the dominant quark–antiquark content as displayed in Fig. 11. We find that the EM mass shift *pattern* (alternating sign) of pseudoscalar mesons can be understood to be largely due to a combination of two dominant effects: (i) a positive chiral Coulombic self–energy part closely related to the pionic system via Dashen's theorem, and (ii) non–chiral contributions of alternating sign, which depend on the ratio of the SU(2) breaking parameter to the SU(3) breaking parameter, in this simple approach. These two contributions reproduce $(\Delta m_\pi^2)^{\frac{1}{2}}$ and $(\Delta m_K^2{}^{\frac{1}{2}})$ typically within several percent, $(\Delta m_D^2)^{\frac{1}{2}}$ within ~ 20% and they predict Δm_B^2 to be large and negative. The results give a rough indication of the expected magnitude of the $O(m_q^3)$ terms in the D– and B– meson systems.

IV Conclusions

The two–flavour NJL model discussed here is the original and simplest version of all NJL–type models. The aim here was to show the extent to which low–energy pion observables can be understood in such a simple but explicit model embedding the most important features of QCD with a minimal number of free parameters. It turns out that the pion is reasonably well described down to distances of ~ 0.3 fm from the origin (the

*) Δm_π^2 is our input value; the NJL model for example can reproduce this value within 5%.

electromagnetic size of the pion is ~ 0.65 fm). The original NJL model is a fully covariant model of the pion without any center–of–mass problems, remarkably different from all quark potential models. The pion starts out as a (massless) Goldstone mode and acquires its observed small hadronic mass by a mass term in the NJL Lagrangian with a $m_{u,d}$ current quark mass of order 5 MeV. The non–renormalizable nature of its 4–Fermion contact interaction requires a 4–momentum cut–off which enforces in a crude way the asymptotic freedom property of QCD. However, the model is not confining its constituent quarks and antiquarks ; this becomes only noticeable for relatively large 4–momentum squares when the absorptive part of the form factor $F_\pi(q^2)$ converges to a constant, resulting in a logarithmically diverging $(\to -\infty)$ $F_\pi(q^2)$ in the space–like region. The Goldstone pion remains massless in higher orders (shown here for the sub–leading order in N_c).

The next order $O(1/N_c^2)$ diagrams involve 3π– intermediate states in the pion self–energy and a momentum dependent quark self–energy which is difficult to solve self–consistently without new approximations. It remains, therefore, to be seen if these next–order loop diagrams can be handled mathematically in a symmetry–preserving way, or if one has to abandon the simplistic contact interaction at this stage in favour of a non–local interaction which will give rise to additional higher order diagrams already at the order in N_c considered here.

Acknowledgement:

I am grateful to Professor Kramer of the II. Inst. f. Theoretische Physik der Univ. Hamburg for fruitful discussions.

References

[1] W.A. Bardeen, C.N. Leung, S.T. Love, "Dilaton and chiral symmetry breaking", Phys. Rev. Lett. **56** (1986) 1230–1233.

[2] N.H. Christ, Nucl. Phys. **A527** (1991) 539.
T.D. Cohen, D.B. Leinweber, Comments Nucl. Part. Phys. **21** (1993) 137.
F. Brandstäter, A.S. Kronfeld, G. Schierholz, Nucl. Phys. **B345** (1990) 709.
S. Aoki, A. Gocksch, Phys. Rev. **D45** (1992) 3845.
M.–C. Chu, M. Lissia, J.W. Negele, Nucl. Phys. **B360** (1991) 31.
M. Lissia, M.–C. Chu, J.W. Negele, J.M. Grandy, Nucl. Phys. **A555** (1993) 272.
R.L. Altmeyer et al., Nucl. Phys. **B389** (1993) 445 and in : Lattice '93, to be publ. in Nucl. Phys. B (Suppl) (1994).

[3] D.B. Leinweber, R.M. Woloshyn, T. Draper, Phys. Rev. **D43** (1991) 1659.
T. Draper, R.M. Woloshyn, W. Wilcox, K. F. Liu, Nucl. Phys. **B318** (1989) 319.

[4] Y. Nambu, Phys. Rev. Lett **4** (1960) 380, Y. Nambu, G. Iona–Lasinio, Phys. Rev. **122** (1961) 345 and **124** (1961) 246.

[5] G. 'tHooft, Phys. Rev. Lett. **37** (1976) 8 and Phys. Rev. **D14** (1976) 3432.

[6] J. Bardeen, L.N. Cooper, J.R. Schrieffer; Phys. Rev. **108** (1957) 1175.

[7] Particle Data Group, M. Aguilar–Benitez et al., Phys. Rev. **D45** (1992) Part 2.

[8] S.P. Klevansky, Rev. Mod. Phys. **64** (1992) 649.

[9] W. Pauli, F. Villars; Rev. Mod. Phys. **21** (1949) 434.

[10] G. 'Hooft, Nucl. Phys. **B62** (1973) 444
G. 't Hooft, Nucl. Phys. **B74** (1974) 461.

[11] V. Dmitrasinovic, R.H. Lemmer, R. Tegen
(a) Phys. Lett. **B284** (1992) 201 and (b) Comments Nucl. Part. Phys. **21** (1993) 71.

[12] A.W. Blin, B. Hiller, M. Schaden, Z. Phys. **A331** (1988) 75.

[13] V. Dmitrasinovic, R.H. Lemmer, R. Tegen
"The pion and quark mass differences in the Nambu and Jona–Lasinio model", preprint (Univ. Witw) 1994.

[14] J. Bijnens et al., "Low–energy behaviour of two–point functions of quark currents", Preprint (Nordita/CNRS/CERN) 1993
J. Bijnens, E. de Rafael, Phys.Lett. **B273** (1991) 483.

[15] J. Gasser, H. Leutwyler, Nucl. Phys. **B250** (1985) 465.

[16] J. Bijnens, Ch. Bruno, E. de Rafael, Nucl. Phys. **B390** (1993) 501.

[17] B. Holstein, Phys. Lett. **B244** (1990) 83

[18] V. Bernard, Phys. Rev. **D34** (1986) 1601.

[19] S.L. Adler, Phys. Rev. **117** (1969) 2426.
J.S. Bell, R. Jackiw, Nuov. Cim. **51** (1969) 47; W.A. Bardeen, Phys. Rev. **184** (1969) 1848.

[20] E. Llanta, R. Tarrach; Phys. Lett. **91B** (1980) 132.

[21] V. Bernard, D. Vautherin; Phys. Rev. **D40** (1989) 1615.

[22] Y.M. Antipov et al., Z. Phys. **C26** (1985) 496.

[23] S. Gerasimov, Sov. J. Nucl. Phys. **29** (1979) 259; R. Tarrach, Z. Phys. **C2** (1979) 221.

[24] S.R. Amendolia et al., Nucl. Phys. **B277** (1986) 168.

[25] J.F. Crawford et al., Phys. Rev. **D43** (1991) 46.

[26] V. Barger, E. Kazes, Nuov. Cim. **28** (1963) 385.

[27] (a) T. Das, et al., Phys.Rev.Lett. **18** (1967) 759.
(b) J. Bijnens, E. de Rafael; Phys.Lett. **B273** (1991) 483.

[28] M.A. Shifman, A.I. Vainshtein, V.I. Zakharov, Nucl. Phys. **B147** (1979) 385 and 447.

[29] R. Dashen, Phys. Rev. **183** (1969) 1245.

[30] J. Bijnens, W.A. Bardeen, J.–M. Gerard, Phys. Rev. Lett. **62** (1989) 1343.

[31] T.–P. Cheng, L.–F. Li, "Gauge Theory of elementary particle physics" Clarendon (1984) Oxford University Press, p. 186ff.
M.D. Scadron, "Advanced Quantum Theory", 2nd ed., Spinger–Verlag (1991).

[32] V. Dmitrasinovic et al., "A chirally symmetric approximation to the NJL model beyond Hartree + RPA". Preprint (Univ. Witwatersrand) 1993.

[33] A. Salam, Nuov. Cim. **25** (1962) 224.
S. Weinberg, Phys. Rev. **130** (1962) 776.

[34] P. Senjanovic Ann. Phys. **100** (1976) 227.
T. Heinzl, S. Krusche, E. Werner, Phys. Lett. **B275** (1992) 410.
W.–M. Zhang, A. Harindranath, Phys. Lett. **B314** (1993) 223.
P. Gaete, J. Gamboa, I. Schmidt, "Path integral approach to two–dimensional QCD in the light–front", preprint Si–93–10/USM–TH–63/IF–(UFRJ)–93–11.

[35] J. Gasser, H. Leutwyler, "Quark masses", Phys. Rep. **87** (1982) 77.

[36] H.M. Pilkuhn: "Relativistic Particle Physics", Springer (1979), New York.

[37] H. Pagels, P. Langacker, Phys. Rev. **D8** (1973) 4620.

[38] R.H. Lemmer, R. Tegen, in preparation.

[39] V. Bernard, U.–G. Meißner, Phys. Lett. **B266** (1991) 403.

[40] M. Lutz, W. Weise; Nucl. Phys. **A518** (1990) 156;U. Vogl., W. Weise, Prog.Part. Nucl.Phys. **27** (1991) 195.

Figure Captions

[1] (a) The quark selfenergy (constituent mass) in the "Hartree" approximation; this is a quadratically divergent graph regularised in a symmetry preserving way within the Pauli–Villars scheme, see text.

(b) The "Fock" term; the solid dots in (a) and (b) represent the 4–Fermion scalar interaction as in the NJL model Lagrangian.

(c) The two–body Schwinger–Dyson equation in the "Random Phase Approximation (RPA)".

(d) The fundamental bubble whose iteration (as in (c)) produces the bound state in the pseudoscalar channel; it is the quark–loop contribution to the pion self–energy.

(e) Quark tadpole contribution to the pion self–energy; it is included in NJL via (a), i.e. the quarks in the loops (d) have a constituent mass m given by the gap equation (a).

[2] Effect of symmetry breaking on the masses of pseudoscalar mesons (schematically), see text.

[3] (a) The weak pion decay amplitude $\pi^{\pm} \to e^{\pm} \overset{(-)}{\nu}$ in lowest order of N_c; this is a logarithmically divergent quark loop for f_π.

(b) The anomalous $\pi^0 \to 2\gamma$ decay amplitude in lowest order of N_c.

[4] Quark loop representation of $\gamma\pi^{\pm} \to \pi^{\pm}$.

[5] Electromagnetic mass shift of the pion at the hadronic level :

(a) the pion–pole term; (b) the "tad–pole" terms.

[6] As in [5] but now at the quark level; note that the tadpole Fig. 5b2 gets a structure as in b2–b4.

[7] Meson loop graphs contributing to m_π^2 to O(1) at the hadronic level.

[8] Same as Fig. [7] but now at the quark level.

[9] Pion electromagnetic form factor at the hadronic level, including meson cloud corrections.

The "sea gulls" in (a) and (b) are not shown but necessary for gauge invariance and included in the calculations.

[10] $O(1/N_c^2)$ corrections to the RPA pion.

(a) Vertex corrections to the $\pi\sigma$–pole term

(b1) "Dressing" of "Hartree" term

(b2) "Dressing" of "Fock" term

(c) "Dressing" of $\pi q\bar{q}$ vertex

(d) "Tower" diagram; corresponds to some $\sigma\pi$–correlation.

[11] SU(6) flavour multiplet: dominant quark–antiquark content of pseudoscalar mesons. The dots stand for possible mixings of π^0, η, η', ..., η_b. None of the T mesons have been identified to date. Also, the B_s and B_c mesons need to be confirmed.

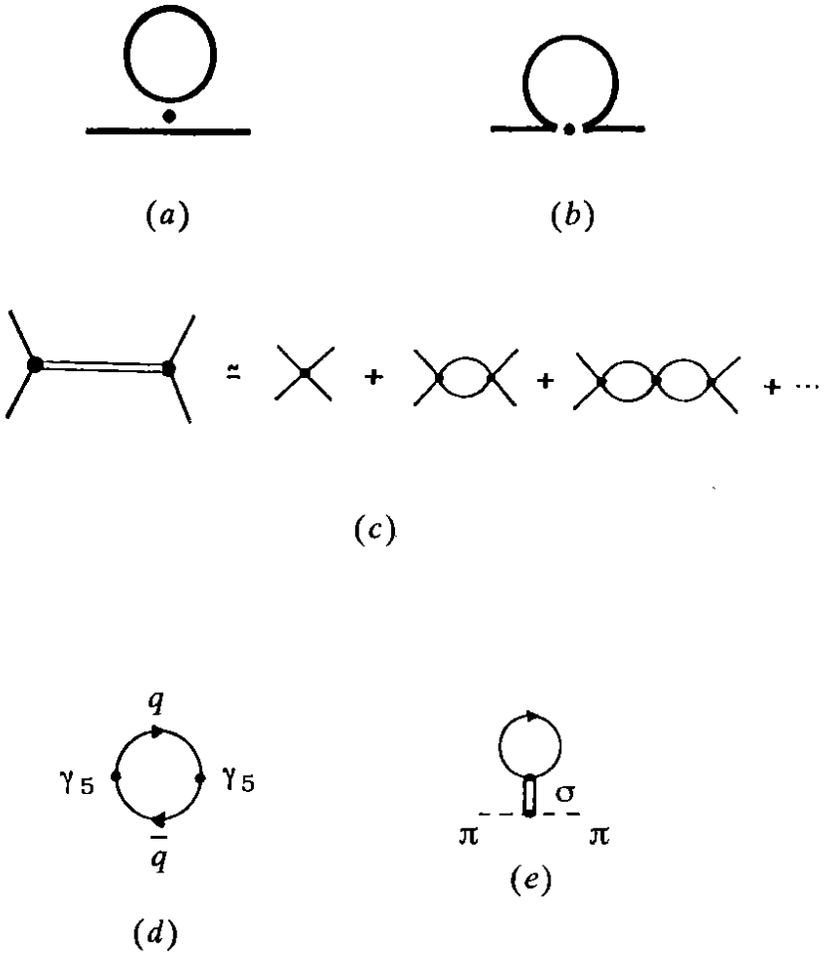
(a)
(b)
≃
+
+
+ ···
(c)
q
γ5
γ5
q̄
(d)
σ
π
π
(e)

*Fig.*1

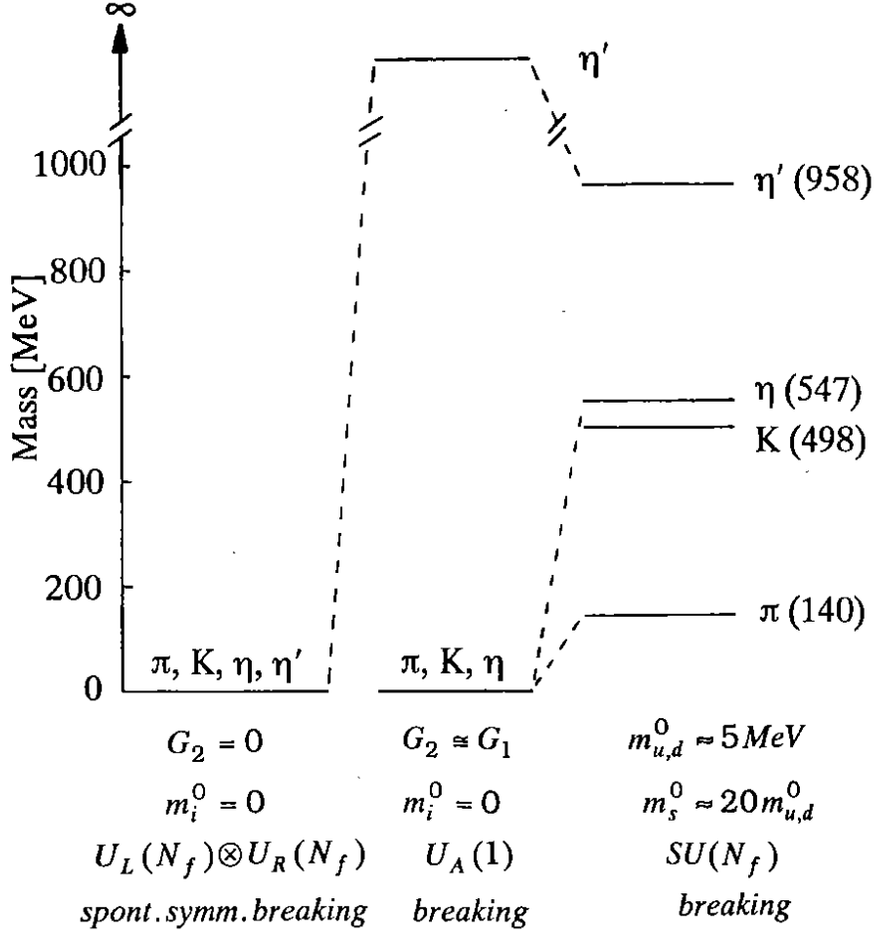
$J^P = 0^-$ Mesons
∞
1000
800
600
400
200
0
Mass [MeV]
η′
η′ (958)
η (547)
K (498)
π (140)
π, K, η, η′
π, K, η
$G_2 = 0$
$m_i^0 = 0$
$U_L(N_f) \otimes U_R(N_f)$
spont. symm. breaking
$G_2 \cong G_1$
$m_i^0 = 0$
$U_A(1)$
breaking
$m_{u,d}^0 \approx 5 MeV$
$m_s^0 \approx 20 m_{u,d}^0$
$SU(N_f)$
breaking

*Fig.*2

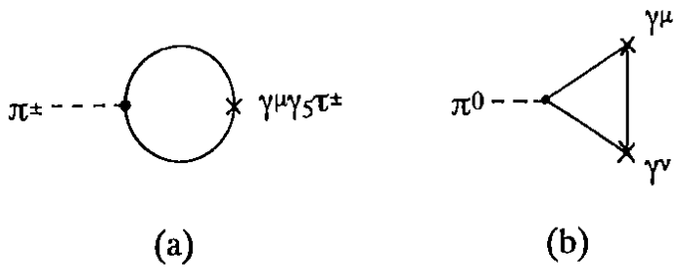

Fig.3

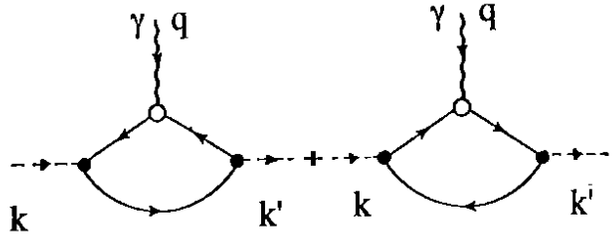

Fig.4

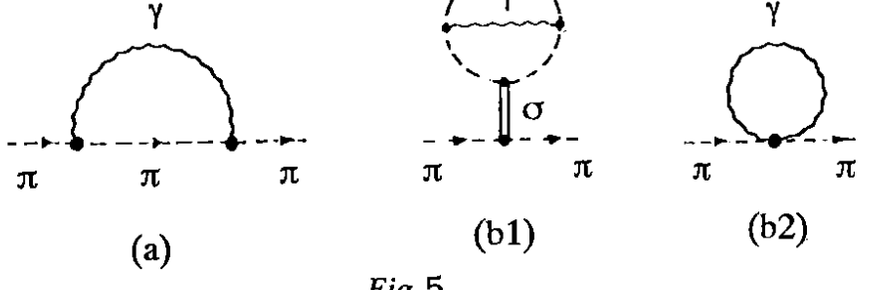

Fig.5

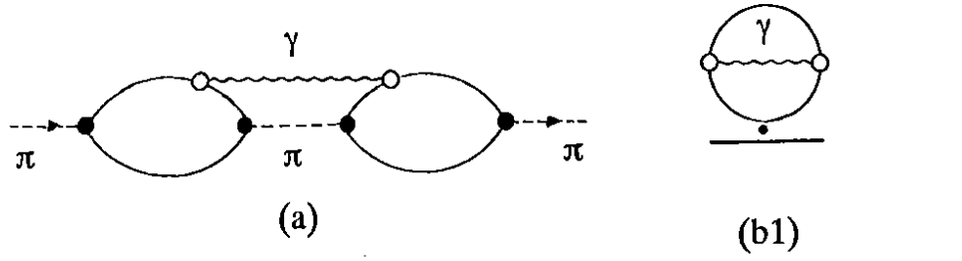

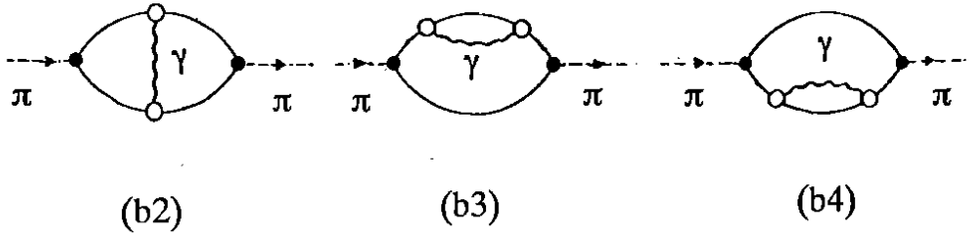

Fig.6

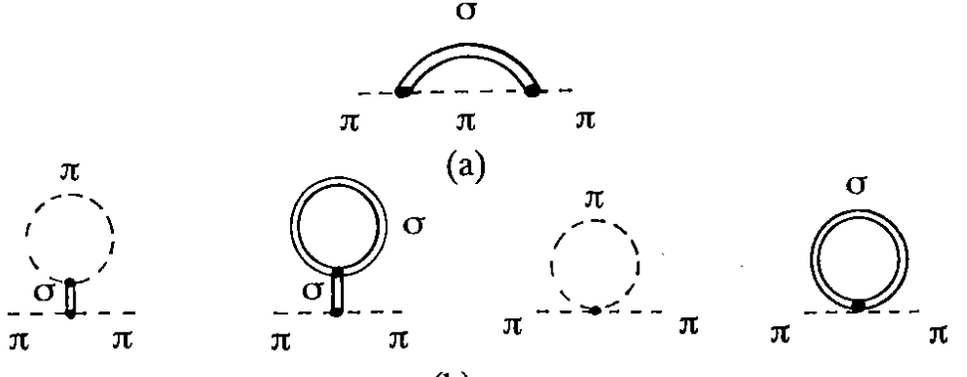

Fig.7

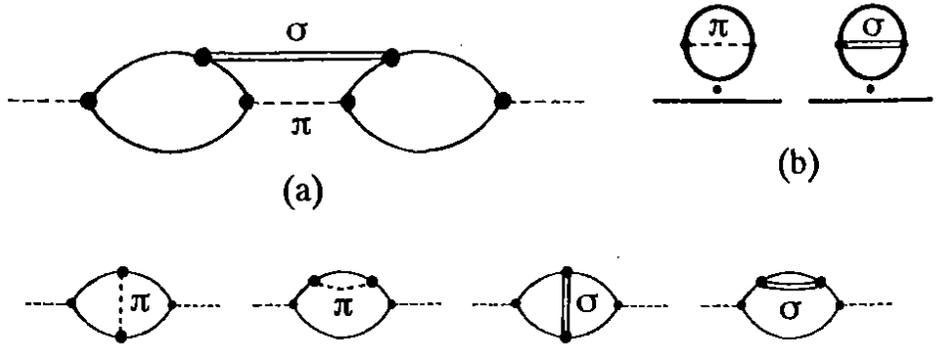

*Fig.*8

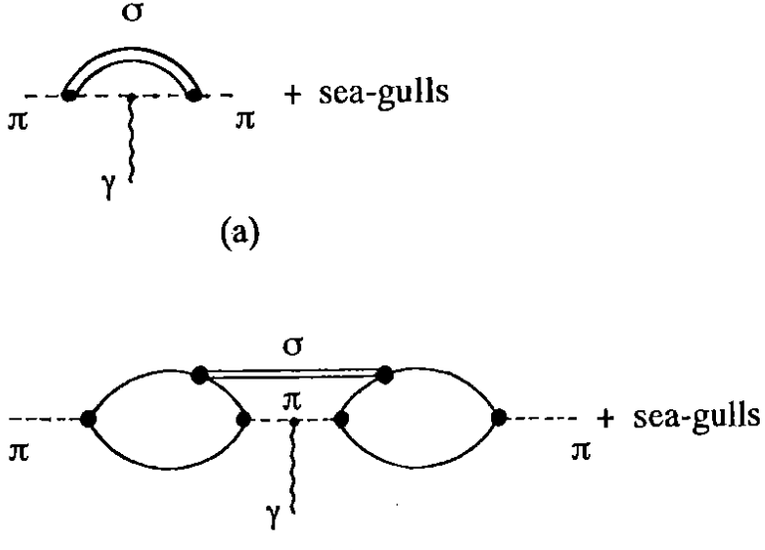

*Fig.*9

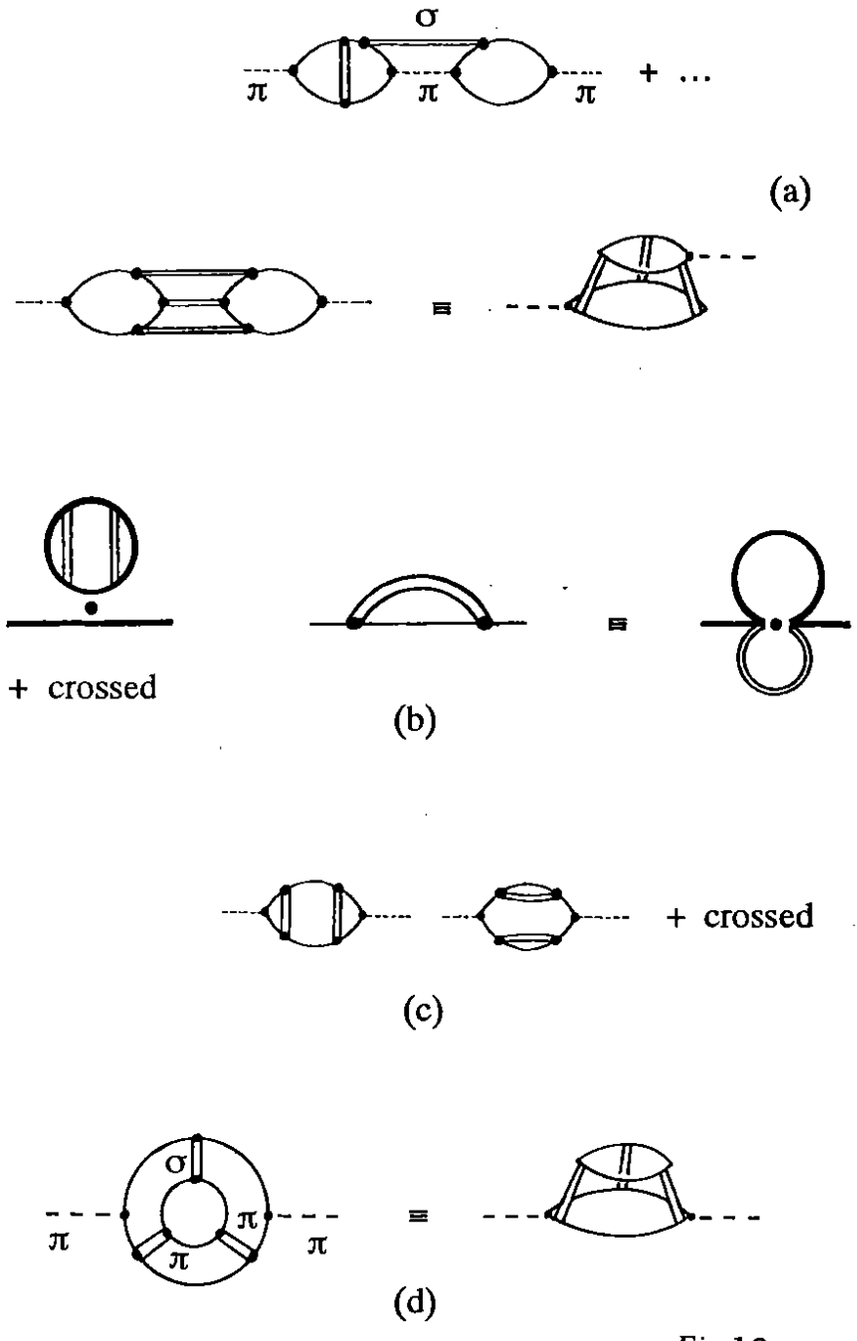

*Fig.*10

	u	d	c	s	t	b
$\bar{u}$	$\pi^0, \eta, \eta', \ldots$	π^-	D^0	K^-	T^0	B^-
$\bar{d}$	π^+	$\pi^0, \eta, \eta', \ldots$	D^+	$\overline{K^0}$	T^+	$\overline{B^0}$
$\bar{c}$	$\overline{D^0}$	D^-	$\eta_c, \ldots$	D_s^-	T_c^0	B_c^-
$\bar{s}$	K^+	K^0	D_s^+	$\eta, \eta', \ldots$	T_s^+	B_s^0
$\bar{t}$	$\overline{T^0}$	T^-	$\overline{T_c^0}$	T_s^-	$\eta_t, \ldots$	T_b^-
$\bar{b}$	B^+	B^0	B_c^+	$\overline{B_s^0}$	T_b^+	$\eta_b, \ldots$

*Fig.*11